Journal of
Petroleum Engineering & Technology
https://journals.stmjournals.com/jopet
ISSN: 2231-1785 (Online)
ISSN: 2321-5178 (Print)
Volume 15, Issue 2, 2025
May–August
DOI (Journal): 10.37591/JoPET
Research JoPET

Utilizing Machine Learning to Evaluate the Connection between Poisson's Ratio and the Petrophysical Properties of Reservoir Rocks

Sudad H. Al-Obaidi[1], Falah H. Khalaf[2], Smirnov Viktor[3,*]

Abstract

The Poisson's ratio is a crucial cornerstone, illuminating our understanding of geomechanical behaviour in wells during the dynamic drilling process and the inspiring recovery journey. This research rigorously employs machine learning methods to analyse the significant impact of geophysical parameters on the Poisson ratio in hydrocarbon reservoirs found in oil fields. The analysis utilized data from multiple oil and gas fields, highlighting the crucial relationships between the Poisson ratio, the natural radioactivity of rocks, and the velocity of the longitudinal wave. Understanding these dependencies is essential for optimizing extraction processes and improving resource management. The PIK-UIDK/PL unit was crucial in conducting triaxial tests on samples in reservoir conditions. The insights gained from these tests have led to essential dependencies that underscore their significance. Numerous geophysical well surveys are utilized to establish robust equations that define the relationship between the Poisson ratio and geophysical parameters. This is achieved through effective linear regression and advanced machine-learning methods. Based on these dependencies, the Poisson ratio can be assessed more accurately for various rocks and fields. In addition to improving efficiency in hydrocarbon production and optimizing oil industry operations, the findings can be used to improve forecasts and modelling for oil field development processes.

Keywords: Poisson's ratio, longitudinal wave, machine learning, petrophysical properties, PIK-UIDK/PL unit

INTRODUCTION

The static Poisson's ratio (ν) is one of the most significant and at the same time the least defined parameter in the calculation of the stress state. The study of the static Poisson's ratio is carried out everywhere during the implementation of almost any project on geomechanics [1–4]. Still, there is no proven method for distributing this parameter along a geological section based on borehole and seismic 3D studies. Therefore, despite the experiments carried out, in most cases, researchers use the dynamic Poisson's ratio, which practically does not change within one lithotype and is used, as a rule, by geophysicists as a characteristic determining the lithofacies composition of the strata [5–8]. At the same time, almost all experts point to the undeniable importance of the static Poisson's ratio in geomechanical calculations, particularly in hydraulic fracturing design [9–12].

At present, neither domestic nor foreign literature contains reliable universal relationships between Poisson's ratio and the parameters most frequently used in geomechanics, such as the elastic modulus, compressive and tensile strength limits, adhesion,

***Author for Correspondence**
Smirnov Viktor
E-mail: vi620929@gmail.com

[1]Professor, Department of Mining, Mining University, St Petersburg, Russia
[2]Professor, Department of Petroleum Engineering, Knowledge University, Erbil, Iraq
[3]Professor, Department of Mining, Scientific Research Center, Russia

Received Date: March 22, 2025
Accepted Date: March 26, 2025
Published Date: April 06, 2025

Citation: Sudad H. Al-Obaidi, Falah H. Khalaf, Smirnov Viktor. Utilizing Machine Learning to Evaluate the Connection between Poisson's Ratio and the Petrophysical Properties of Reservoir Rocks. Journal of Petroleum Engineering & Technology. 2025; 15(2): 33–43p.

internal friction angle, and longitudinal and transverse wave velocities [13–16]. There are relationships for individual deposits that cannot be extended even to neighbouring deposits due to the low tightness of the relationship between the obtained relationships. One reason for the lack of reliable dependencies is the complexities in determining this parameter, which is regulated by various domestic and international standards.

According to Method for Determining Deformation Characteristics under Uniaxial Compression, you can determine the deformation characteristics of rocks only when they are tested in a uniaxial mode [17–20]. ASTM standards describe uniaxial and triaxial tests [21, 22], and ISRM recommendations have separate documents on determining strength under triaxial loading [23, 24]. Many methods do not contain information on determining deformation characteristics. The issue of the difference in determining elastic parameters under uniaxial and triaxial loading is not considered in these methods.

According to literature, tests are carried out to determine the modulus of elasticity, Poisson's ratio, deformation modulus, and transverse deformation coefficient [25–28]. It is indicated that these characteristics should be defined in the range of required stresses from 5 to 50% of the ultimate strength under uniaxial compression.

The ISRM and ASTM methodologies state that the modulus of elasticity can be determined using any method employed in engineering practice and outline several more commonly used techniques [29–32]. The first option is the tangential modulus of elasticity, determined at a fixed level from the ultimate strength (usually 50% of the ultimate strength in uniaxial compression). The second is the average modulus of elasticity on the linear portion of the stress-strain diagram. The third option is the secant modulus, determined at a fixed level from the tensile strength (also usually 50%). Poisson's ratio is calculated based on the ratio of the axial-to-radial deformation in the section where the elastic modulus is determined. ASTM standards state that elastic moduli can be calculated directly and by the best approximation of the section of the stress-strain diagram, which is under consideration by a straight line using the least squares method.

Thus, the spread of methods for determining the loading section of the sample, where the elastic modulus and Poisson's ratio are located, can lead to a significant difference in the parameters being set. And if this is not so significant for the elastic modulus due to its large boundaries, from several to hundreds of GPa, then for Poisson's ratio, a difference of 0.1 leads to the impossibility of obtaining reliable correlation dependencies.

Review of Previously Obtained Dependencies

It should be noted that in some cases it is possible to obtain relatively stable dependencies on individual geophysical parameters, primarily on the longitudinal wave velocity and the parameter characterizing the natural radioactivity of the section. Figure 1 shows the dependence of the static Poisson's ratio of sandstones and siltstones of oil fields in the Perm Territory on the intensity of gamma radiation [33, 34]. As we can see, the distribution of the Poisson's ratio along the productive section of the object can be constructed based on the intensity of gamma radiation of terrigenous rocks.

Figure 2 shows a similar dependence of the Poisson ratio of productive formations of the Sarmatskoye oil field on the indicator characterizing the natural radioactivity of rocks. Samples for testing are represented by various lithotypes (argillites, dolomites, clayey limestone, etc.). A pattern was revealed when the test results were processed: the Poisson ratio for argillite in reservoir conditions reaches 0.35, and it does not exceed 0.25 for limestone. Moreover, the lower the clay content, the lower the Poisson ratio. Based on this, an attempt was made to determine the relationship between the static Poisson ratio and wells' gamma-ray logging (GR) data. As a result, for all tested samples in three wells, a relationship was built between the static Poisson's ratio and the GR data with a fairly high indicator of the tightness of the relationship. It should be noted that in earlier studies, a relationship was found between the Poisson's ratio and the volume content of clays for the Adamtash deposit (Central Asia), as well as with the intensity of gamma radiation in sandstones, siltstones, and argillites, which is determined by the content of clay minerals [35–38].

Figure 3 shows the dependence of Poisson's ratio on the longitudinal wave velocity for samples of productive objects of the Salmanovskoye gas condensate field. The samples are represented by formations with average occurrence depths of 900 m (PK_{1-9}), 1600 m (XM_{6-10}) and 1600–2900 m (TP). As can be seen from the graph, the dependence is characterized by a relatively low connection (R^2=0.42). Note that this dependence can be used for approximate calculations of lateral rock pressure.

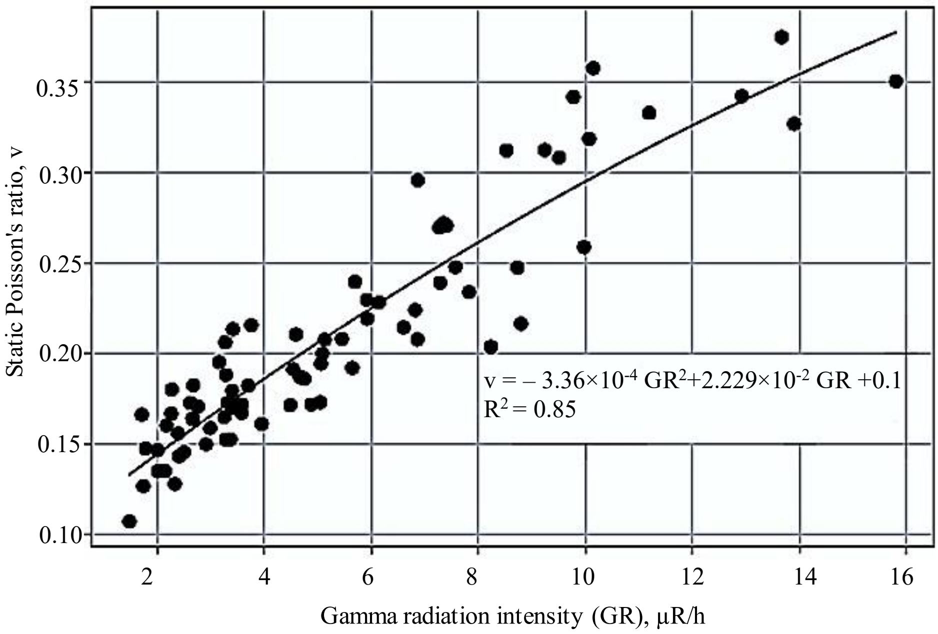

Figure 1. Dependence of the static Poisson's ratio of sandstones and siltstones of oil fields in the Perm region on the intensity of gamma radiation.

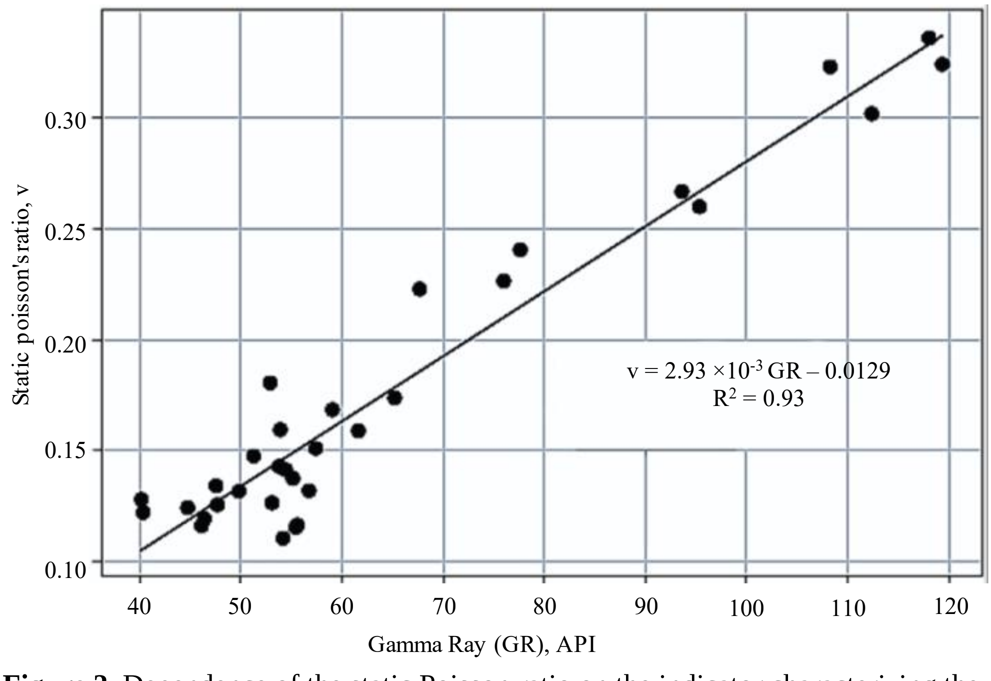

Figure 2. Dependence of the static Poisson ratio on the indicator characterizing the natural radioactivity of rocks.

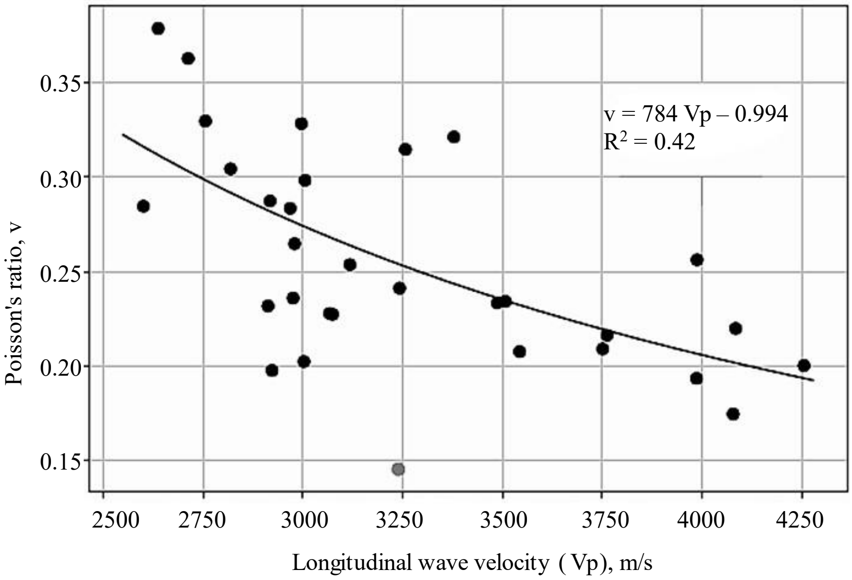

Figure 3. Dependence of Poisson's ratio of samples of objects (formations) of the Salmanovskoye deposit on the velocity of the longitudinal wave. The point highlighted in red is excluded when constructing the dependence.

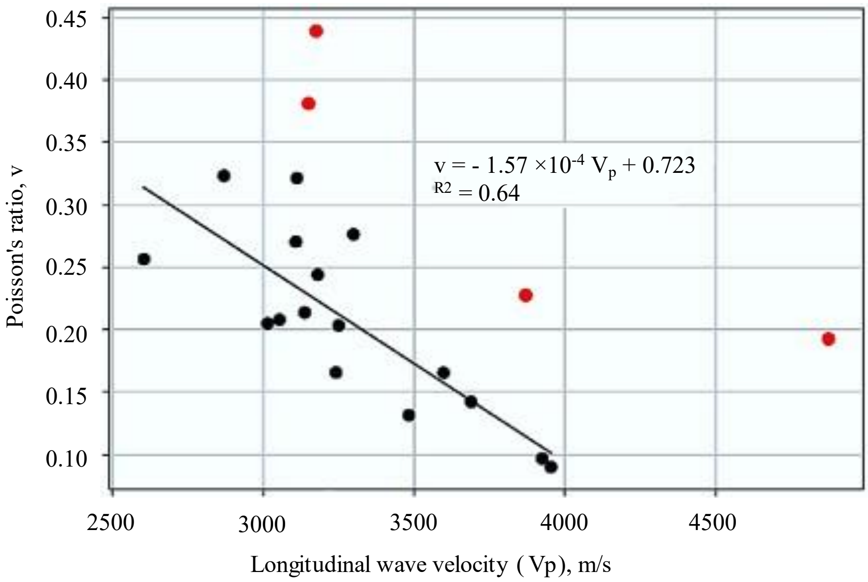

Figure 4. Dependence of Poisson's ratio of Bazhenov sediment samples of the Sredne-Nazymskoye field, oriented perpendicular to the bedding, on the velocity of the longitudinal wave. The points highlighted in red are excluded when constructing the dependence.

A similar dependence is typical for samples of Bazhenov deposits of the Sredne-Nazymskoye field, oriented perpendicular to the bedding. Most samples have longitudinal wave velocity Vp values in the range of 2500–4000 m/s. For this section, Figure 4 shows the dependence of Poisson's ratio on Vp. The points excluded from the construction of dependencies are marked in red in Figures 3 and 4. They may be outliers for the following reasons: significant heterogeneities in the samples, the influence of other factors unrelated to the longitudinal wave velocity, etc.

Thus, for individual deposits, the dependences of the Poisson ratio on the longitudinal wave travel speed and the GR log parameter are constructed. However, it is not possible to obtain sufficiently reliable dependences for a group of deposits using conventional statistical methods (Figure 4).

Due to the limited dependencies of the Poisson ratio on the geological, geophysical, and geomechanical characteristics of the section, individual researchers are exploring the relationship between geophysical parameters and the Poisson ratio using machine learning techniques [39–42]. This study presents the results of similar studies using machine learning to establish the dependence of the Poisson ratio on the geophysical characteristics of the studied sections of Western Urals deposits.

METHODOLOGY AND MATERIALS

Finding Dependencies Using Machine Learning Methods

A total of 156 tests were conducted on different sections of the Western Urals deposits; however, due to an uncertain signal when determining the longitudinal wave velocity, some samples were excluded from the final analysis. The final selection consisted of 145 samples. It contains samples of both terrigenous and carbonates rocks.

Triaxial compression experiments were performed on the unique scientific installation PIK-UIDK/PL. The tests were conducted at effective pressure; pore pressure was not specified. The effective pressure corresponding to reservoir conditions was calculated by considering the dependencies for the Biot coefficient previously obtained [43–46]. Axial loading and unloading were performed with a constant rate of axial deformations, the same for all experiments, which was 10^{-5} s^{-1}. The rate of change of lateral pressure did not exceed 1 MPa/min.

The general program of triaxial testing of samples for elastic properties under reservoir conditions consists of the following stages:

- Loading the sample to a specific all-around pressure that matches the reservoir conditions for the given sample.
- Holding the sample until volumetric deformations stabilize:

$$\frac{\partial \varepsilon_{vol}}{\partial t} = 0 \quad (1)$$

- Measurement of longitudinal and transverse wave velocities *Vp, Vs.*
- Production of two sample loading/unloading cycles by creating an axial load without exceeding the elastic limit.

Obtaining the straightest possible line on the stress-strain graph on the load branch determines a sufficient load level. The elastic deformation limit is taken to be the bend in the curve in the axes "axial load"-"volume deformations". Volume deformations are calculated as the sum of axial and radial deformations.

Continuous recording of axial stress, axial and transverse deformations, and all other parameters is carried out throughout the experiments.

The results of all tests were reprocessed using a single method to exclude the influence of some processing features, such as the section size for determining elastic parameters. Differences may arise if different people process the test results at different times. Additional parameters, including the load level for determining elastic parameters, were also obtained for plotting the dependence of Poisson's ratio.

RESULTS AND DISCUSSION

The elastic modulus and Poisson's ratio were calculated on the straight sections of the branches of the repeated loading of the sample on the diagram "axial stresses-deformations" in the region of elastic deformations. An example of the diagram of the deformation of the sample with the indication of the section for determining the elastic parameters is shown in Figure 5.

The dynamic elastic moduli and Poisson's ratio were determined from the velocities of longitudinal and transverse waves under reservoir conditions using established relationships [47–50].

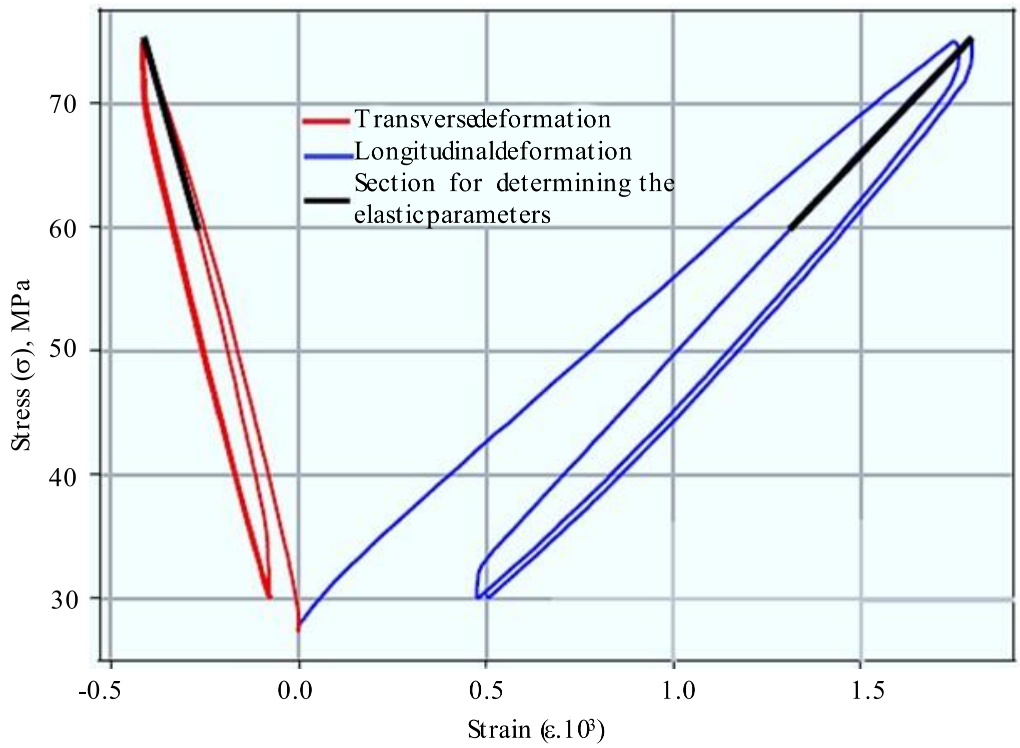

Figure 5. Example of a sample deformation diagram indicating the area for determining elastic parameters.

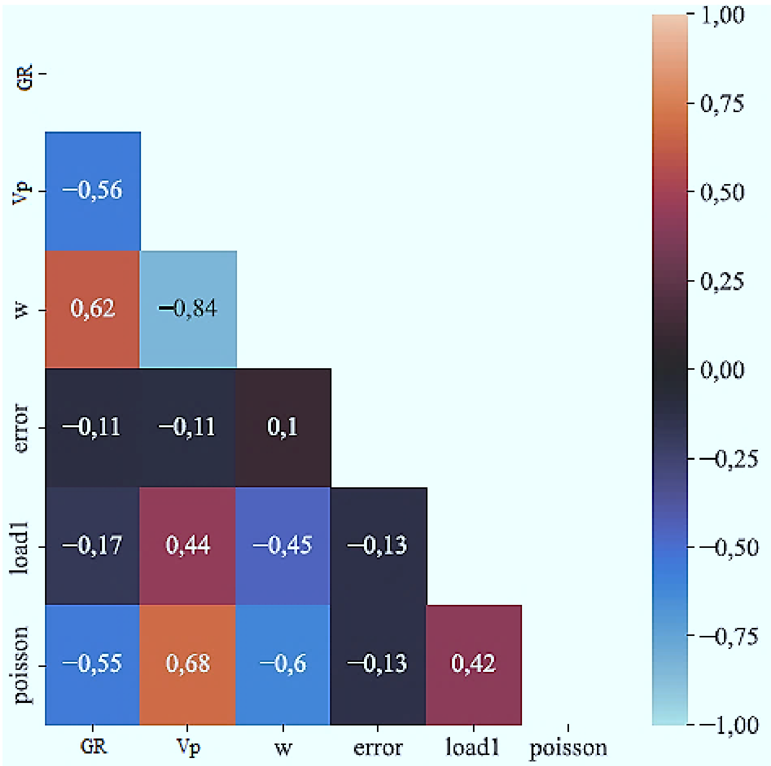

Figure 6. Heat map of pair correlations: GR: gamma ray, vp: propagation velocity of longitudinal wave, w: hydrogen content, error: error in determining Poisson's ratio, load1: load at which it was determined, poisson: Poisson's ratio.

The next step in data preparation for training involves selecting parameters and refining them into the required format. The parameters chosen for training were the well-logging data obtained throughout the wellbore, which can potentially be normalized. Before utilizing the well-logging data, it was essential to normalize them collectively. However, before normalization, the data needed to be adjusted for a more accurate comparison with the results from point tests.

Figure 6 shows a heat map of pairwise correlation coefficients, which shows all the selected parameters, their cross-correlations, and their correlations with the Poisson ratio. It is clear that, for parameters with low correlation coefficients with the Poisson ratio, their cross-pairwise correlations are quite high in absolute terms, which is not always acceptable when applying machine learning methods.

In regression analysis, multicollinearity is critical because it affects the model's ability to distinguish between unique values of the regression coefficients, which can distort their estimates. Small changes in the data used for estimation can cause large fluctuations in the estimated coefficients. This creates difficulties with inference: if two variables are highly correlated, a change in one variable can be offset by a change in the other, cancelling their effect. In gradient optimization methods, an unlimited increase in the model weights is also possible, which makes the search for optimal parameters of the optimization function impossible. In this case, it was decided to exclude the hydrogen content (*w*), as the parameter most correlated with acoustics (*Vp*), while having a lower correlation coefficient value with the target parameter. The analysis also used the *GR*, errors in determining the Poisson ratio when approximating a section of the curve with a straight line (*error*) and the load at which it was determined (*load1*) were taken into account.

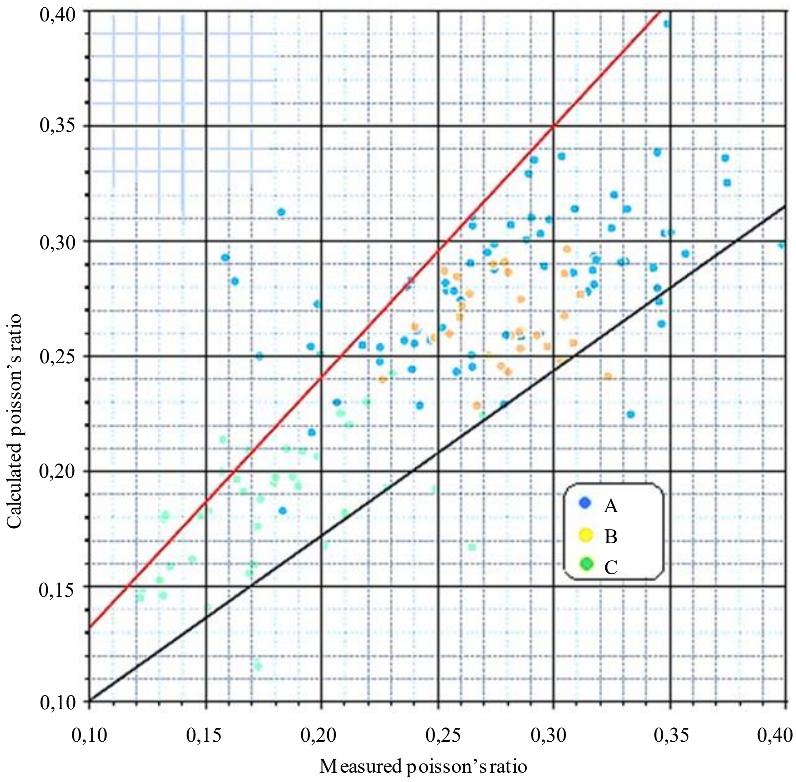

Figure 7. Comparison of Calculated vs. Measured Poisson's Ratio for Material Sets A, B, and C. Cross-plot of the determined from tests (measured Poisson's ratio) and calculated Poisson's ratio for terrigenous and carbonate productive objects of the Western Urals deposits: A: Tournaisian stage of the lower section of the Carboniferous system together with the Famennian stage of the upper section of the Devonian system, B: Tulskian and Bobrikovian horizons of the Visean stage of the lower section of the Carboniferous system, C: Bashkirian stage of the middle section of the Carboniferous system.

The search for a relationship was carried out using linear regression with the Huber loss function, which allows for excluding outliers. Various combinations of the parameters shown in Figure 6 were used as input parameters. The parameters were added to the model one by one, after which the model was retrained and the cross-validation error was estimated. Parameters were added until the error significantly decreased. The final cross-plot is shown in Figure 7. The resulting equation included the longitudinal wave travel speed and GR data in various variations.

The error in determining the Poisson ratio (*error*), which was present in the regression model, is taken to be zero in the resulting equation. The correlation coefficient of the resulting regression dependence was 0.74, which is a good result in this case (for such an uncertain parameter). Figure 7 shows the cloud of obtained values, according to which confidence intervals were constructed.

The lower confidence interval estimate should be used as the final result since it is the best approximation of the experiment's drained conditions. Such conditions imply a sufficiently low loading rate at which the sample's pore pressure does not increase. Under undrained conditions, the liquid does not have time to flow out of the sample due to low permeability or a high rate of load application.

The equation for the Poisson ratio, obtained from the lower confidence interval estimate, is:

$$v = 2.34x10^{-5}V_p - 6.14x10^{-2}Ln(GR+1) + 3.29x10^{-10}V_p^2 GR + 0.166 \quad (2)$$

Where *GR* is the natural radioactivity of rocks determined using *GR log, μR/h,* V_P is the longitudinal wave velocity determined using well logging, *m/s.*

Thus, using machine learning methods and processing heterogeneous test data using a single methodology, it is possible to obtain fairly stable correlations between the Poisson ratio and the geophysical characteristics of the productive section.

CONCLUSION

The studies conducted lead us to the following conclusions:

Currently, there are no reliable dependencies of the Poisson ratio on the geomechanical and geophysical characteristics of productive objects. One reason is the lack of a strict, standardized method for determining this parameter.

For specific productive types of deposits, correlations have been identified that connect the deposit properties with the velocity of longitudinal waves, the natural radioactivity of rocks, and the clay content. However, these correlations do not apply to other types of deposits.

This study proposes a machine learning-based method for establishing the Poisson ratio's dependence on the main geophysical parameters of the geological section. With this method, the correlation dependencies of this parameter on the longitudinal wave velocity and the GR data were obtained for terrigenous and carbonate-producing objects of the Western Urals deposits. The correlation coefficient of the obtained regression dependence was 0.74, which is a good result.

REFERENCES

1. Tao Z, *et al*. A physical modeling-based study on the control mechanisms of Negative Poisson's ratio anchor cable on the stratified toppling deformation of anti-inclined slopes. Int J Rock Mech Min Sci. 2021; 138: 104632. https://doi.org/10.1016/j.ijrmms.2021.104632.
2. Obaidi SH, Chang WJ. Techniques to Boost Oil Production in the Development of Multi-Reservoir Fields. J Earth Environ Waste Manag. 2024; 2(3): 1–7.
3. Kamensky IP, Al-Obaidi SH, Khalaf FH. Scale effect in laboratory determination of the properties of complex carbonate reservoirs. Int Res J Mod Eng Technol Sci. 2020; 2(11): 1–6.

4. Al-Obaidi SH, Patkin AA, Guliaeva NI. Advance Use for the NMR relaxometry to investigate reservoir rocks. J Petrol Eng Technol. 2003; 2(3): 45–48.
5. Descamps F, et al. Relationships between geomechanical properties and lithotypes in NW European chalks. Geol Soc Lond Spec Publ. 2017; 458: SP458.9. https://doi.org/10.1144/SP458.9.
6. Al-Obaidi S. Investigation of rheological properties of heavy oil deposits. In: Conference of the Arabian Journal of Geosciences. Cham: Springer Int Publ; 2019; 399–402.
7. Miel H, Hameed AO, Hussein KF. Modeling and monitoring the development of an oil field under conditions of mass hydraulic fracturing. Trends Sci. 2022; 19(8): 3436–3436.
8. Al-Obaidi SH, Kamensky IP, Hofmann M. Changes in the physical properties of hydrocarbon reservoir as a result of an increase in the effective pressure during the development of the field. engrXiv. 2010.
9. Truong TV, *et al.* Prediction of Poisson's ratio for hydraulic fracturing operations in the Oligocene formations in the Bach Ho field. J Min Earth Sci. 2024; 65(6): 47–57. https://doi.org/10.46326/JMES.2024.65(6).05.
10. Al-Obaidi SH. Experimental study of the influence of fluid flow rate on the risk of rock destruction. Jo Pet Eng Emerg Technol. 2009; 9(4): 84–89.
11. Chang WJ, Al-Obaidi S, Smirnov VI. Application of multi-stage hydraulic fracturing (MSFH) in the development of deep-lying deposits with low permeability of hydrocarbon fields. J Geol Geophys. 2023; 12: 1154.
12. Al-Obaidi S. Analysis of hydrodynamic methods for enhancing oil recovery. J Petrol Eng Technol. 2007; 6(3): 20–26.
13. Gonzaga GG, Leite MH, Corthésy R. Determination of anisotropic deformability parameters from a single standard rock specimen. Int J Rock Mech Min Sci. 2008; 45(8): 1420–1438. https://doi.org/10.1016/j.ijrmms.2008.01.014.
14. Al-Obaidi SH, Khalaf FH. Acoustic logging methods in fractured and porous formations. J Geol Geophys. 2017; 6(4): 2.
15. Hofmann M, Al-Obaidi SH, Chang WJ. Evaluation Of Quantitative Criteria for Triassic Reservoirs in the South Mangyshlak Basin. Nat Sci Adv Technol Educ. 2023; 32(1): 7–24.
16. Al-Obaidi SH, Guliaeva NI. Determination of flow and volumetric properties of core samples using laboratory NMR relaxometry. J Petrol Eng Technol. 2002; 1(2): 20–23.
17. Xie WQ, *et al*. A review of test methods for uniaxial compressive strength of rocks: Theory, apparatus and data processing. J Rock Mech Geotech Eng. 2025; 17(3): 1889–1905. https://doi.org/10.1016/j.jrmge.2024.05.003.
18. Al-Obaidi SH, Khalaf FH, Alwan HH. Performance analysis of hydrocarbon wells based on the skin zone. Technium. 2021; 3(4): 50–56.
19. Smirnov VI, Al-Obaidi S. Innovative methods of enhanced oil recovery. Oil Gas Res. 2008; 1(1): e101.
20. Al-Obaidi SH, Chang W. Evaluation of the Quantitative Criteria of Triassic Carbonate Rocks Reservoirs. J Geol Geophys. 2023; 12: 1067.
21. ASTM D3967-16. Standard test method for splitting tensile strength of intact rock core specimens. ASTM. 2023; Vol. 04.08:5. Available from: https://doi.org/10.1520/D3967–16.
22. Al-Obaidi SH. Calculation Improvement of the Clay Content in the Hydrocarbon Formation Rocks. Oil Gas Res. 2017; 3(1): 130.
23. Muralha J, Grasselli G, Tatone B, et al. ISRM suggested method for laboratory determination of the shear strength of rock joints: Revised version. Rock Mech Rock Eng. 2014; 47: 291–302. Available from: https://doi.org/10.1007/s00603-013-0519-z.
24. Khalaf FH, Al-Obaidi SH. The Effects of Hydro Confining Pressure on the Flow Properties of Sandstone and Carbonate Rocks. Int J Sci Technol Res. 2018; 7(2): 283–286.
25. Cózar IR, JJ, *et al*. A novel methodology to measure the transverse Poisson's ratio in the elastic and plastic regions for composite materials. Compos Part B Eng. 2024; 272: 111098. Available from: https://doi.org/10.1016/j.compositesb.2023.111098.

26. Al-Obaidi S, Smirnov VI, Khalaf F. New technologies to improve the performance of high water cut wells equipped with ESP. Technium. 2020; 3(1): 104–113.
27. Chang WJ, Al-Obaidi SH, Patkin AA. The use of oil-soluble polymers to enhance oil recovery in hard-to-recover hydrocarbons reserves. Int Res J Mod Eng Technol Sci. 2021; 3(1): 982–987.
28. Al-Obaidi SH, Chang WJ, Khalaf FH. Determination of the Upper Limit Up to Which the Linear Flow Law (Darcy's Law) Can Be Applied. J Xidian Univ. 2021; 15(6): 277–286.
29. Aladejare AE. Evaluation of empirical estimation of uniaxial compressive strength of rock using measurements from index and physical tests. Journal of Rock Mechanics and Geotechnical Engineering. 2020 Apr 1;12(2):256–68.
30. Al-Obaidi SH, Hofmann M, Smirnov VI, Khalaf FH, Alwan HH, *et al.* A study of compositions relevant to selective water isolation in gas wells. J Geol Geophys. 2021; 10(7): 1000.
31. Patkin A, Al-Obaidi SH. Influence of temperature and pressure of incoming oil-containing liquid from field wells on the gas separation process. J Pet Eng Emerg Technol. 2001; 3(4): 20–24.
32. Al-Obaidi SH. High oil recovery using traditional water-flooding under compliance of the planned development mode. J Pet Eng Technol. 2016; 6(2): 48–53.
33. Kashnikov YUA, Ashihmin SG. Rock mechanics in petroleum industry. Moscow: Gornaya kniga; 2019; 496.
34. Al-Obaidi SH, Khalaf FH. A new approach for enhancing oil and gas recovery of the hydrocarbon fields with low permeability reservoirs. Pet Petro Chem Eng J. 2023; 7(2): 000343. Available from: https://doi.org/10.23880/ppej–16000343.
35. Hussain W, Luo M, Ali M, Al-Khafaji H, Hussain I, Hussain M, Ahmed S, Ullah O. A Gamma-ray spectroscopy approach to evaluate clay mineral composition and depositional environment: A case study from the lower Goru Formation, Southern Indus Basin, Pakistan. J Appl Geophys. 2024; 226: 105414. Available from: https://doi.org/10.1016/j.jappgeo.2024.105414.
36. Al-Obaidi SH. Improve the efficiency of the study of complex reservoirs and hydrocarbon deposits – East Baghdad field. Int J Sci Technol Res. 2016; 5(8): 129–131.
37. Galkin A, *et al*. Dependences of reservoir oil properties on surface oil. Jo Pet Eng Emerg. 2005; 5(9): 74–77.
38. Al-Obaidi SH, Hofmann M. A study on how permeability heterogeneity influences initial water cut in undersaturated oil formations. Nat Sci Adv Technol Educ. 2024; 33(5–6): 347–361. Available from: https://doi.org/10.53656/nat2024-5-6.03.
39. Riyadi ZA, *et al*. Machine learning prediction of permeability distribution in the X field Malay Basin using elastic properties. Results Eng. 2024; 24: 103421. Available from: https://doi.org/10.1016/j.rineng.2024.103421.
40. Al-Obaidi SH, Chang WJ, Hofmann M. Development of oil fields using science artificial intelligence and machine learning. Nat Sci Adv Technol Educ. 2023; 32(3–4):187–200. Available from: https://doi.org/10.53656/nat2023-3-4.01.
41. Alexander G, Sudad AO, Viktor S. Numerical simulation of water alternating gas injections (WAG) into hydrocarbon reservoirs: Factors influencing oil recovery. J Geol Geophys. 2023; 12: 1147.
42. Al-Obaidi SH, Khalaf FH. The effect of anisotropy in formation permeability on the efficiency of cyclic water flooding. Int J Sci Technol Res. 2017; 6(11): 223–6.
43. Nolte S, Fink R, Krooss BM, Littke R. Simultaneous determination of the effective stress coefficients for permeability and volumetric strain on a tight sandstone. J Nat Gas Sci Eng. 2021; 95: 104186. doi:10.1016/j.jngse.2021.104186.
44. Al-Obaidi SH, Galkin AP. The assessment of reservoir pressure and recoverable hydrocarbon reserves using production well research data. J Geol Min. 2025; 2(1): 1–6.
45. Hofmann M, Al-Obaidi SH, Chang WJ. Evaluating the efficacy of water alternating gas injection technique in the Upper Jurassic hydrocarbon reservoirs, considering saturation pressure. Nat Sci Adv Technol Educ. 2024; 33(3–4): 237–250. doi:10.53656/nat2024-3-4.02.
46. Al-Obaidi SH, Wang JC, Hofmann M. Modelling the development of oil rim using water and gas injection. Nat Sci Adv Technol Educ. 2022; 31(3): 279–92.

47. Shen S, Gao Y, Jia L. A comparison of the relationship between dynamic and static rock mechanical parameters. Appl Sci. 2024; 14(11): 4487. doi:10.3390/app14114487.
48. Al-Obaidi SH, Kamensky IP. Express study of rheological properties and group composition of oil and condensate using nuclear magnetic resonance–relaxometry. J Oil Gas Coal Technol. 2022; 4(1): 102.
49. Chang WJ, Al-Obaidi SH, Patkin AA. The use of oil-soluble polymers to enhance oil recovery in hard-to-recover hydrocarbons reserves. Int Res J Mod Eng Technol Sci. 2021; 3(1): 982–7.
50. Al-Obaidi SH. Enhancing hydrocarbon field recovery: Employing multi-stage hydraulic fracturing (MSHF) for the development of low-permeability deep-lying deposits. J Geol Earth Mar Sci. 2023; 1(1): 102.